Modelling inertial effects in periodic fluid–structure systems with an homogenisation approach: Application to seismic analysis of tube bundles

Daniel Broc, Jean-François Sigrist

Modelling inertial effects in periodic fluid–structure systems with an homogenisation approach: Application to seismic analysis of tube bundles

Daniel Broc [a], Jean-François Sigrist [b,*]

[a] CEA, DEN, DANS, DM2S, SEMT, F-91191 Gif-sur-Yvette, France
[b] Département Dynamique des Structures, DCNS Research, 44620 La Montagne, France

Fluid–structure interaction (FSI) is of major importance when describing the dynamic behaviour of nuclear pressure vessels, since the presence of confined fluid strongly influences the response of structures when subjected to external loadings, such as a seismic loading. Accounting for FSI when performing the seismic analysis of nuclear reactors or steam generators can be done through the description of inertial effects, which are predominant in the low frequency domain. Finite element techniques are now of common use in design office to model coupled (quiescent) fluid–structure systems, using standard non-symmetric ($\mathbf{u}$,p) or symmetric ($\mathbf{u}$,p,φ) coupled formulations. When con-sidering complex systems such as a tube bundle in steam generators, producing a finite element model which includes tubes, fluid and structures is a tedious task which is out of reach in many practical applications. A homogenisation method has been proposed which allows FSI modelling of tube bundles: it has been successfully applied to a complex structure. In the aforementioned developments, focus was put on the mathematical and numerical aspects of the method, leaving out some questions regarding the physical interpretation of the calculations. In the present paper, a new insight on the homogenisa-tion approach is exposed with the objective of proposing a formulation of the method based on physical considerations, leading to a correction of the homogenised problem. Enhancement of the method is discussed from an engineering standpoint: it allows for a wider range of applications in the nuclear industry.

1. Introduction

Fluid–structure interaction (FSI) is of major importance when describing the dynamic behaviour of nuclear pressure vessels, since the modal characteristics of such systems are strongly affected by the fluid, whether in flowing conditions (De Ridder et al., 2013) or in a quiescent state (Sigrist and Garreau, 2007). FSI formulations have been developed and implemented in many finite element codes (Morand and Ohayon, 1995). They are in particular applied for the numerical modelling of nuclear components which are subjected to external loading, such as occurring in a seismic event. However, "classical" FSI methods are sometimes not applicable in practice, when the system under concern has a complex geometry, such as steam generators. Describing FSI within tube bundles by coupling fluid and structure finite element methods is

* Corresponding author. Tel.: +33 2 40 84 87 84; fax: +33 2 40 84 79 94.
E-mail addresses: jean-francois.sigrist@dcnsgroup.com, jfsigrist@wanadoo.fr (J.-F. Sigrist).

Nomenclature

Γ	fluid/structure interface
Δ	direction of dynamic loading
$\varepsilon(\mathbf{u}_\Sigma)$	structure strain field
μ_n	effective mass
ρ_Σ, ρ	structure, fluid density
$\sigma(\mathbf{u}_\Sigma)$	structure stress field
Σ	structure domain
φ	fluid displacement potential field
$\mathbf{\Phi}$	fluid displacement potential degrees of freedom
ω_n	eigenpulsation
Ω	fluid domain
Ω_S	tube elementary domain
Ω_F	fluid elementary domain
Ω_T	elementary cell domain
B_S	confinement ratio
c	fluid acoustic wave velocity
$\mathbf{C}$	fluid/tubes interaction matrix
$\mathbf{K}$	system stiffness matrix
$\mathbf{K}_\Sigma, \mathbf{K}_S, \mathbf{K}_F$	structure, tubes and fluid stiffness matrices
$\mathbf{M}$	system mass matrix
$\mathbf{M}_\Sigma, \mathbf{M}_S, \mathbf{M}_F$	structure, tubes and fluid mass matrices
p	fluid pressure field
$\mathbf{P}$	fluid pressure degrees of freedom
$\mathbf{R}$	fluid/structure interaction matrix
$\mathbf{u}_F, \ddot{\mathbf{u}}_F$	fluid local displacement/acceleration field
$\mathbf{U}_F, \ddot{\mathbf{U}}_F$	fluid global displacement/acceleration field
$\mathbf{u}_S, \ddot{\mathbf{u}}_S$	tube displacement/acceleration field
$\mathbf{u}_\Sigma$	structure displacement field
$\mathbf{U}_\Sigma, \mathbf{U}_S$	structure, tubes displacement degrees of freedom
$\mathbf{X}_n$	eigenmode

obviously not possible as regards the number of degrees of freedom at stake. Alternative approaches, such as homogenisation of the periodic fluid–structure system, have been proposed to tackle this issue.

Homogenisation methods have been developed and applied in various fields for structures with periodic geometry, for instance for composite media (Bensoussan et al., 1978), for fluids in porous media (Sanchez-Palencia, 1980) and for fluid–structure coupled problems (Conca et al., 1995). In power nuclear engineering, such approaches have been applied for fluid–structure interaction modelling in reactor cores (Broc et al., 2003; Brochard et al., 1987a; Cheval, 2001; Zhang, 1998a; Zhang et al., 2001), in reactor internals (Brochard et al., 1987b) and in fuel assemblies (Schumann, 1981; Shinohara-Shimogo, 1981; Planchard, 1985a, 1985b) or tube bundles (Hammami, 1991; Jacquelin et al., 1996; Planchard, 1987; Zhang, 1999, 1998b). In these studies, two-dimensional as well as three-dimensional applications of homogenisation techniques have been considered (Brochard et al., 1996). Using a homogenisation method for FSI modelling in tube bundle configuration enables the description of both the tubes and fluid system through an equivalent continuous media, thus avoiding the tedious task to mesh all structure and fluid sub-domains within the tube bundle (Sigrist and Broc, 2007a).

Recently, Broc and Sigrist proposed an engineering approach of homogenisation techniques to account for fluid–structure interaction in reactor internals (Sigrist and Broc, 2007b) and in tube bundles (Sigrist and Broc, 2008a, 2008b). The method is based on the following hypotheses.

- Modelling of fluid–structure interaction is restricted to inertial effects, i.e. displacements of the tubes are assumed small with respect to the dimension of the bundle, and the fluid is considered incompressible and inviscid. Compressibility effect in the fluid can be discarded when the first coupled frequencies and the pure acoustic frequencies are well dissociated. As detailed by Veron et al. (2014) and as evidenced further on, a formulation of the homogenised fluid–structure with compressibility effects in the fluid is possible, so that vibro-acoustic coupling can be accounted for.
- The fluid–structure system exhibits a repetitive pattern, i.e. accelerations of the tubes are supposed to undergo small variations from one cell to another, and interactions between neighbouring tubes are not taken into account.

Although validated on simple test cases and applied to industrial-like structures (Sigrist and Broc, 2009), some questions regarding the physical interpretation of the calculations were left unanswered. In addition some limits of the method have been highlighted, for instance, when describing the behaviour of high frequency coupled eigenmodes. As it might be of importance to correctly describe the contribution of such modes, particularly when modelling non-linear effects (impact between tubes for example), this shortcoming is still to be tackled in order to allow applications to a broader range of industrial problems. In such context, the aim of the paper is i) to propose a new insight of the homogenisation approach, focusing on both the mathematical and the physical standpoints (Section 2), ii) to highlight and discuss the existing shortcomings of the method with a physical point of view (Section 3), and iii) to propose an appropriate correction of the method in order to solidify its application (Section 4).

2. Inertial effects in a periodic tubes and fluid system

2.1. Homogenisation methods

Reduced Order Modelling (ROM) receives a growing attention for various engineering applications since it allows for the design of computationally efficient numerical simulations of multi-physics problems, such as FSI (Gallardo et al., 2014).

Among ROM techniques, homogenisation methods can be used to model heterogeneous systems, such as coupled fluids and solids. The variety of such approaches is beyond the scope of the present paper; it can however be simply stated that homogenisation derives from the following hypothesis.

- *Double scale asymptotic development*: When the problem exhibits a geometrical periodicity, it is convenient to divide the domain into identical cells with a typical length period ε which is supposed to be "small" in comparison to the characteristic length of the system. Denoting by φ the problem unknowns and supposing φ to be ε-dependent, one writes $\varphi_\varepsilon = \varphi_o + \sum_{k\geq 1}\varepsilon^k \varphi_k(X,x)$, where functions φ_k depend on the "local scale" variable x and the "global scale" variable X (with $x = X/\varepsilon$).
- *Term-to-term identification*: Substituting the former expression of φ into the partial differential equations which represent the fluid–structure system and performing term-to-term identification yields a set of multi-scale problems for φ_k. In addition, an averaging process is required to formulate the equations for the "mean problem" φ_o.
- *Closure condition*: For periodic systems, the multi-scale and the "mean problems" are to be solved in an elementary cell, which yields the "homogenised model".

The "homogenisation method" under concern in the present paper does not follow this rigorous development. Adopting a straightforward approach, it solely lies on an average process over an elementary cell. Despite this simplification, such an approach is found to be of engineering relevance. The underlying principles of the method are detailed in various preceding publications. They are summarised below, adopting a physical viewpoint.

2.2. Elementary cell analysis

As the geometry of tube bundle systems is characterised by periodicity/symmetry conditions it is possible to identify an elementary cell, which is representative of the tube confinement. As depicted in Fig. 1, Ω_S and Ω_F stand for the tube and fluid domain, $\Omega_T = \Omega_S \cup \Omega_F$ is the elementary cell; Γ_T, Γ_S and Γ_F denote the cell, the tube and the fluid boundaries.

For the homogenisation approach discussed here, it is assumed that the tube/fluid dynamics at the "local scale" can be described by a two degrees of freedom system, namely through the acceleration (or displacement) of the tube, denoted as $\ddot{\mathbf{u}}_S$ (or $\mathbf{u}_S$), and the mean acceleration (or displacement) of the cell, denoted as $\ddot{\mathbf{U}}_F$ (or $\mathbf{U}_F$). The latter is defined as

$$\ddot{\mathbf{U}}_F = \frac{|\Omega_S|}{|\Omega_T|}\ddot{\mathbf{u}}_S + \frac{1}{|\Omega_T|}\int_{\Omega_F} \ddot{\mathbf{u}}_F \, d\Omega_F, \tag{1}$$

where $\ddot{\mathbf{u}}_F$ stands for the acceleration of the fluid.

Highlighting the physical interpretation of Eq. (1) is as follows:

- $(1/|\Omega_F|)\int_{\Omega_F} \ddot{\mathbf{u}}_F \, d\Omega_F = \overline{\ddot{\mathbf{u}}}_F$ is the mean acceleration of the fluid within the fluid domain,
- $|\Omega_T|\ddot{\mathbf{U}}_F \cdot \mathbf{e}_i$ is the mean fluid flux through the cell boundary along direction $\mathbf{e}_i$.

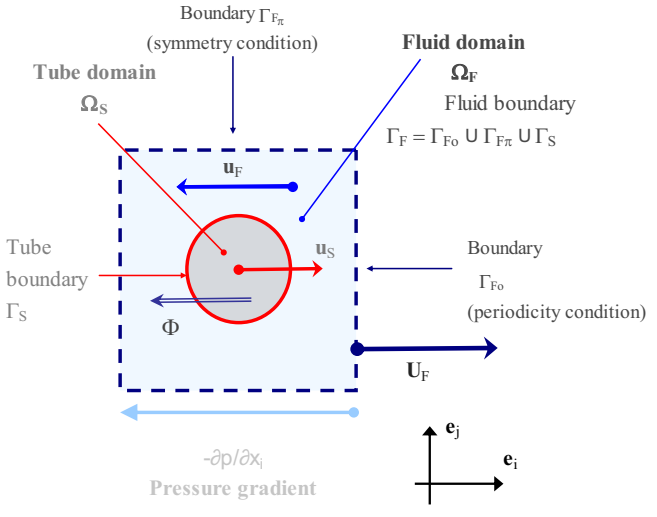

Fig. 1. Elementary cell: single tube in array confinement.

The latter is indeed defined as $\int_{\Gamma_T} x_i \ddot{\mathbf{u}} \cdot \mathbf{n}\, d\Gamma_T$, which can be equivalently calculated as $\int_{\Omega_T} \nabla \cdot (\ddot{\mathbf{u}} x_i) d\Omega_T$ according to the divergence theorem. Since $\nabla \cdot (\ddot{\mathbf{u}} x_i) = \ddot{u}_i\, \nabla x_i + x_i \nabla \cdot \ddot{u}_i = \ddot{\mathbf{u}} \cdot \mathbf{e}_i$ when considering an incompressible flow ($\nabla \cdot \ddot{u}_i = 0$), one writes

$$\int_{\Gamma_T} x_i \ddot{\mathbf{u}} \cdot \mathbf{n}\, d\Gamma_T = \int_{\Omega_T} \ddot{\mathbf{u}} \cdot \mathbf{e}_i\, d\Omega_T = |\Omega_S| \ddot{\mathbf{u}}_S \cdot \mathbf{e}_i + |\Omega_F| \overline{\ddot{\mathbf{u}}}_F \cdot \mathbf{e}_i = |\Omega_T| \ddot{\mathbf{U}}_F \cdot \mathbf{e}_i,$$

which is Eq. (1).

Using $\ddot{\mathbf{u}}_S$ and $\ddot{\mathbf{U}}_F$ as degrees of freedom of the elementary problem, the fluid force applied to the tube is

$$\boldsymbol{\Phi} = -m_a \ddot{\mathbf{u}}_S + (m_a + \rho\ |\Omega_S|) \ddot{\mathbf{U}}_F, \tag{2}$$

with m_a being the added mass of the tube within the cell confinement. The latter expression of the fluid force accounts for FSI only through inertial effect. As will be highlighted in Section 3.1, m_a is obtained from a simple calculation on the elementary cell.

Considering a non-viscous incompressible flow, one can write the equation of motion of the fluid in the elementary cell as

$$\int_{\Omega_F} \rho \ddot{\mathbf{u}}_F\, d\Omega_F = \boldsymbol{\Pi} - \boldsymbol{\Phi},$$

since the fluid is subjected to the force applied by the tube ($-\boldsymbol{\Phi}$) and the pressure forces $\boldsymbol{\Pi}$; the latter is calculated from the pressure gradient $\boldsymbol{\Pi} = -|\Omega_T| \nabla p$, where $|\Omega_T|$ is the elementary cell volume (see notations of Fig. 1).

Using Eqs. (1) and (2) in the fluid momentum conservation equation leads to

$$\rho \ddot{\mathbf{U}}_F = -(1 - B_S) \nabla p + \rho B_S \ddot{\mathbf{u}}_S, \tag{3}$$

where B_S is the confinement ratio of the tube in the elementary cell, given by

$$B_S = \frac{m_a + \rho |\Omega_S|}{m_a + \rho (|\Omega_S| + |\Omega_T|)}. \tag{4}$$

As conveyed by Eq. (1), the flux of the fluid passing through the cell boundary originates from the acceleration of the tube and the pressure gradient. These sources of motion have opposite actions and are balanced by the confinement ratio: the proposed model is equivalent to fluid flow model in porous media.

Using Eq. (1), the expression for the fluid force on the tube can also be reformulated as

$$\boldsymbol{\Phi} = -\rho (B_S |\Omega_T| - |\Omega_S|) \ddot{\mathbf{u}}_S - B_S |\Omega_T| \nabla p,$$

or

$$\boldsymbol{\Phi} = -m_a^* \ddot{\mathbf{u}}_S - B_S |\Omega_T| \nabla p, \tag{5}$$

with $m_a^* = \rho (B_S |\Omega_T| - |\Omega_S|)$.

Eq. (3) is the starting point of the homogenisation approach, since it relates the pressure gradient and the tube acceleration to the mean cell acceleration (as defined by Eq. (1)). $B_S = 0$ indicates that the elementary cell is filled by the fluid only. In this case, Eq. (3) yields the classical relation between fluid acceleration and pressure gradient $\rho \ddot{\mathbf{U}}_F = -\nabla p$. $B_S = 1$ indicates that the elementary cell is filled by the solid only and Eq. (3) gives $\ddot{\mathbf{U}}_F = \ddot{\mathbf{u}}_S$, the physical meaning of which is obvious.

Using $\ddot{\mathbf{U}}_F$ and $\ddot{\mathbf{u}}_S$ as degrees of freedom for the tubes and fluid systems is straightforward since any situation is a linear combination of the two situations depicted in Fig. 2. In both cases, the periodicity condition is imposed on the left hand side and right end side of the cell, while the symmetry condition is imposed on the top and bottom sides. The pressure is therefore constant along both left and right lateral boundaries.

- In the first situation depicted in Fig. 2(a), the fluid flows around the tube which is supposed to be at rest within the cell ($\ddot{\mathbf{u}}_S = 0$). The resulting global motion of the fluid is constant ($\ddot{\mathbf{U}}_F = \gamma$) and the pressure gradient within the cell is $\nabla p = -(\rho\gamma/(1 - B_S))$. On the left hand side, the high level of pressure triggers the fluid motion.
- In the second situation depicted in Fig. 2(b), the tube is accelerated, $\ddot{\mathbf{u}}_S = \gamma$, and generates fluid motion within the cell. At the local scale, the fluid gains acceleration ($\ddot{\mathbf{u}}_F \neq 0$); the mean fluid acceleration is negative ($\overline{\ddot{\mathbf{u}}}_F < 0$), while the tube acceleration is positive. As a result, the mean acceleration represented by Eq. (1) is null ($\ddot{\mathbf{U}}_F = 0$). The pressure gradient within the cell is $\nabla p = \rho B_S \gamma/(1 - B_S)$. High pressure at the right hand side fosters the fluid motion. It is worth emphasizing that in such a case, the global flux between two adjacent cells is null, while locally some fluid flows from one cell to another.

Using $\mathbf{U}_F$ or $\ddot{\mathbf{U}}_F$ as the degree of freedom for the fluid is also more versatile than using $\mathbf{u}_F$ or $\ddot{\mathbf{u}}_F$. Indeed, as $\dot{\mathbf{U}}_F$ stands for the fluid velocity flux at the elementary cell boundary, continuity conditions between two adjacent cells are enforced in a simple manner with $\mathbf{U}_F$. As a consequence, various configurations encountered in many industrial applications can be easily dealt with, see Fig. 3 for illustration.

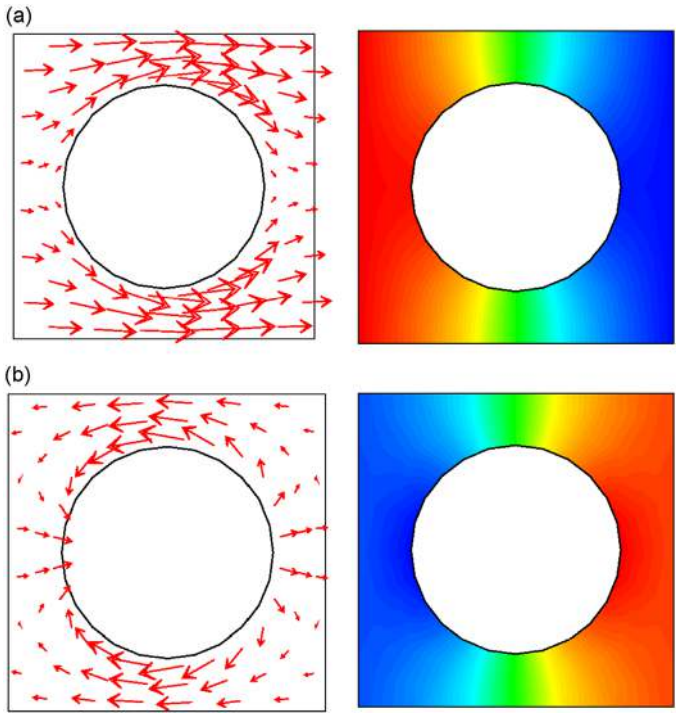

Fig. 2. Elementary cell: a two degrees of freedom system (acceleration and pressure field in the fluid): (a) flowing fluid ($\ddot{\mathbf{U}}_F = \gamma > 0$) with tube at rest ($\ddot{\mathbf{u}}_S = 0$) and (b) moving tube ($\ddot{\mathbf{u}}_S = \gamma > 0$) without fluid "globally flow" ($\ddot{\mathbf{U}}_F = 0$).

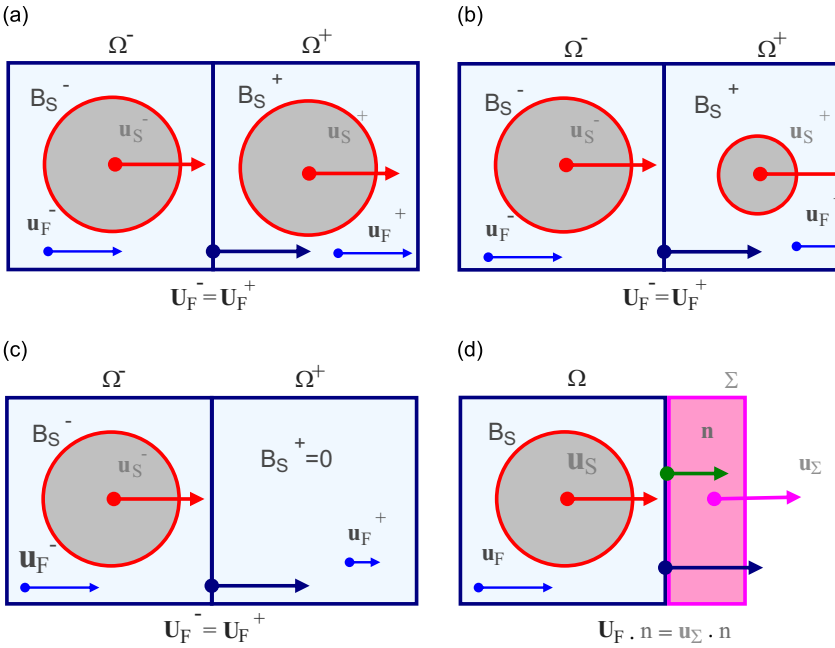

Fig. 3. Various configurations possibly encountered in steam generator and handled by the homogenisation method: (a) two identical adjacent cells, (b) Two different adjacent cells, (c) Two adjacent cells with/without tube, and (d) cell coupled with elastic structure.

2.3. Global behaviour of a structure, tubes and fluid system

Eq. (3) can be used to describe a homogenised domain which contains both tubes and fluid. The general case is schematically represented by Fig. 4. It deals with an elastic structure Σ which is coupled with the homogenised domain Ω, the latter containing the fluid and tubes.

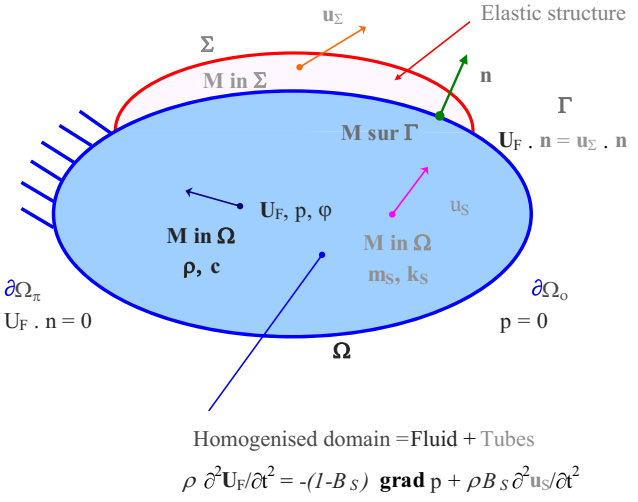

Fig. 4. General case: coupled structure, tubes and fluid system.

Let $\mathbf{u}_\Sigma$ be the structure displacement, $\mathbf{u}_S$ the tube displacement and p the fluid pressure. Following Sigrist and Broc (2008a), it can be stated that the weighted integral formulation of the structure, tubes and fluid coupled problem reads

$$\int_\Omega \frac{\ddot{p}\,\delta p}{\bar{c}^2} d\Omega + \int_\Omega \rho(1-B_S)\nabla p \cdot \nabla\,\delta p\, d\Omega + \int_\Gamma \rho\delta p \ddot{\mathbf{u}}_\Sigma \cdot \mathbf{n}\, d\Gamma - \int_\Omega \rho B_S \ddot{\mathbf{u}}_S \nabla\,\delta p\, d\Omega = 0, \tag{6}$$

for any pressure test function δp (fluid), and

$$\begin{aligned} &\int_\Sigma \rho_\Sigma \ddot{\mathbf{u}}_\Sigma \cdot \delta\mathbf{u}_\Sigma d\Sigma + \int_\Sigma \sigma(\mathbf{u}_\Sigma)\cdot\varepsilon(\delta\mathbf{u}_\Sigma) d\Sigma + \int_\Omega m_S \ddot{\mathbf{u}}_S \cdot \delta\mathbf{u}_S\, d\Omega + \int_\Omega k_S \mathbf{u}_S\, \delta\mathbf{u}_S\, d\Omega \\ &\quad = \int_\Gamma p\mathbf{n}\cdot\delta\mathbf{u}_\Sigma\, d\Gamma + \int_\Omega \rho(|\Omega_S|/|\Omega_T| - B_S)\ddot{\mathbf{u}}_S \cdot \delta\mathbf{u}_S\, d\Omega - \int_\Omega B_S\, \nabla p \cdot \delta\mathbf{u}_S\, d\Omega \end{aligned} \tag{7}$$

for any displacement test functions $\delta\mathbf{u}_\Sigma$ (structure) and $\delta\mathbf{u}_S$ (tubes).

As suggested by Eq. (6), compressibility effects are accounted for with the equivalent speed of sound in the cell: $\bar{c} = c\sqrt{|\Omega_F|/|\Omega_T|}$, where c denotes the speed of sound in the fluid without tubes.

According to Sigrist and Broc (2008a) and Veron et al. (2014), finite element discretisation of the preceding equations yields

$$\begin{bmatrix} \mathbf{M}_S + \mathbf{M}_S^* & \mathbf{0} & \mathbf{0} \\ \mathbf{0} & \mathbf{M}_\Sigma & \mathbf{0} \\ -\rho B_S \mathbf{C}^{\mathrm{T}} & \rho\mathbf{R}^{\mathrm{T}} & \overline{\mathbf{M}}_F \end{bmatrix} \begin{Bmatrix} \ddot{\mathbf{U}}_S(t) \\ \ddot{\mathbf{U}}_\Sigma(t) \\ \ddot{\mathbf{P}}(t) \end{Bmatrix} + \begin{bmatrix} \mathbf{K}_S & \mathbf{0} & B_S\mathbf{C} \\ \mathbf{0} & \mathbf{K}_\Sigma & \mathbf{R} \\ \mathbf{0} & \mathbf{0} & (1-B_S)\mathbf{K}_F \end{bmatrix} \begin{Bmatrix} \mathbf{U}_S(t) \\ \mathbf{U}_\Sigma(t) \\ \mathbf{P}(t) \end{Bmatrix} = \begin{Bmatrix} \mathbf{0} \\ \mathbf{0} \\ \mathbf{0} \end{Bmatrix}. \tag{8}$$

$\mathbf{M}_\Sigma$ and $\mathbf{K}_\Sigma$ are the mass and stiffness matrices of the structure, $\mathbf{M}_S$ and $\mathbf{K}_S$ are the mass and stiffness matrices of the tubes, $\overline{\mathbf{M}}_F$ and $\mathbf{K}_F$ are the "mass" and "stiffness" matrices of the fluid. $\mathbf{R}$ is the fluid/structure interaction matrix, which describes the coupling of the fluid and the structure, as defined in Axisa and Antunes (2006). Additional operators arise from the homogenisation approach (Sigrist and Broc, 2008a):

- $\mathbf{C}$ is the tube/fluid interaction operator, which describes the interaction between the fluid and the tubes,
- $\mathbf{M}_S^*$ is the tube added mass operator, which accounts for an additional inertial effect on tubes, as a consequence of the fluid confinement within the elementary cell.

Using the pressure/displacement formulation yields non-symmetric matrices, as highlighted by Eq. (8). From the engineering standpoint, it can be more convenient to use a pressure–displacement potential/displacement formulation, which leads to symmetric operators (for recall, the displacement potential field is related to the pressure field in the fluid domain according to the relation $p = -\rho(\partial^2\varphi/\partial t^2)$).

As shown in Sigrist and Broc (2008b), the symmetric formulation of the structure, tubes and fluid systems reads

$$\begin{bmatrix} \mathbf{M}_S + \mathbf{M}_S^* & \mathbf{0} & \mathbf{0} & -\rho B_S\mathbf{C} \\ \mathbf{0} & \mathbf{M}_\Sigma & \mathbf{0} & \rho\mathbf{R} \\ \mathbf{0} & \mathbf{0} & \mathbf{0} & \overline{\mathbf{M}}_F \\ -\rho B_S\mathbf{C}^{\mathrm{T}} & \rho\mathbf{R}^{\mathrm{T}} & \overline{\mathbf{M}}_F & -\rho(1-B_S)\mathbf{K}_F \end{bmatrix} \begin{Bmatrix} \ddot{\mathbf{U}}_S(t) \\ \ddot{\mathbf{U}}_\Sigma(t) \\ \ddot{\mathbf{P}}(t) \\ \ddot{\mathbf{\Phi}}(t) \end{Bmatrix} + \begin{bmatrix} \mathbf{K}_S & \mathbf{0} & \mathbf{0} & \mathbf{0} \\ \mathbf{0} & \mathbf{K}_\Sigma & \mathbf{0} & \mathbf{0} \\ \mathbf{0} & \mathbf{0} & 1/\rho\overline{\mathbf{M}}_F & \mathbf{0} \\ \mathbf{0} & \mathbf{0} & \mathbf{0} & \mathbf{0} \end{bmatrix} \begin{Bmatrix} \mathbf{U}_S(t) \\ \mathbf{U}_\Sigma(t) \\ \mathbf{P}(t) \\ \mathbf{\Phi}(t) \end{Bmatrix} = \begin{Bmatrix} \mathbf{0} \\ \mathbf{0} \\ \mathbf{0} \\ \mathbf{0} \end{Bmatrix}. \tag{9}$$

It is worth mentioning that the formulation of the coupled problem given by Eqs. (6) and (7) is consistent with the "classical" pressure/displacement formulation of a coupled fluid–structure system as developed in Morand and Ohayon (1995). In particular, potential energy of the fluid is accounted for in the above equations, through the mass matrix $\overline{\mathbf{M}}_F$

calculated with the equivalent speed of sound. However, this latter contribution will be omitted in the following, as the application of the method will be restricted to the description of inertial effects. From a practical point of view, this will be achieved in numerical simulations with finite elements by setting $c > 10^{+6}$ m/s to model the fluid incompressibility.

3. Physical discussion on a simple fluid–tube system

3.1. 10×10 two-dimensional tube bundle

An application of the homogenisation method is first proposed: it is restricted to a simple 2D case. Note that additional test cases for 2D and 3D problems are presented by Sigrist and Broc (2008a, 2008b, 2007a) and confirm the applicability of the method. Dynamic analysis of a compact steam generator with fluid–structure interaction modelling is shown by Sigrist and Broc (2009).

The test case under concern here consists of a tube bundle embedded in a circular structure. The tube and fluid geometry and physical properties are defined in Fig. 5: $m_l = 4.58$ kg, $k_l = 100$ N/m, $R = 1.35$ cm, and $\rho = 1000$ kg/m^3. The radius of the outer structure is $R' = 1.05(LR/\sqrt{2}) = 2.23$ m ($L = 10$ is the number of tubes and R is the radius of a single tube). The pitch to diameter ratio is $T/2R = 90\%$ (where $T = 3$ cm is the tube spacing), which corresponds to a rather confined tube bundle. The outer bundle structure is of negligible mass ($m_\Sigma \ll m_l$) and of large stiffness ($k_\Sigma \gg k_l$) in comparison to, respectively, the tube mass and stiffness.

All tubes have identical mass and stiffness and have two degrees of freedom. Without fluid, the tubes system has therefore 200 eigenmodes with the same eigenfrequency $f_o = (1/2\pi)\sqrt{k/m}$ and same effective mass $\mu_o = m_l$ in both x and y directions. It is recalled that the effective mass μ_n of eigenmode $\mathbf{X}_n$ in direction Δ is calculated as $\mu_n = (\mathbf{X}_n^T M \boldsymbol{\Delta})^2 / \mathbf{X}_n^T \mathbf{M} \mathbf{X}_n$, where $\mathbf{M}$ denotes the mass matrix of the system. It is also recalled that the total mass of the system can be calculated according to $m = \boldsymbol{\Delta}^T M \boldsymbol{\Delta} = \sum (\mathbf{X}_n^T M \boldsymbol{\Delta})^2 / \mathbf{X}_n^T \mathbf{M} \mathbf{X}_n = \sum \mu_n$.

A finite element mesh for the elementary cell is produced in order to evaluate the confinement ratio (see Fig. 6). This latter is calculated by solving the elementary problem $\Delta p = 0$ in Ω_F, with the following boundary conditions (according to the definitions of Fig. 1):

- $\partial p / \partial n = -\rho \boldsymbol{\gamma} \cdot \mathbf{n}$ on Γ_S (coupling with the tube),
- $\partial p / \partial n = 0$ on $\Gamma_{F\pi}$ (outer boundary of the elementary cell with symmetry condition),
- $p = 0$ on Γ_{Fo} (outer boundary of the elementary cell with periodicity condition).

The elementary cell calculation yields the fluid force on the tube $\boldsymbol{\Phi}$ and the fluid acceleration $\ddot{\mathbf{u}}_F$. $\ddot{\mathbf{U}}_F$ is first evaluated using the equation $\ddot{\mathbf{U}}_F = (|\Omega_S|/|\Omega_T|)\boldsymbol{\gamma} + (1/|\Omega_T|)\int_{\Omega_F} \ddot{\mathbf{u}}_F \, d\Omega_F$. The added mass is then calculated using $\boldsymbol{\Phi}$ and $\ddot{\mathbf{U}}_F$ according to $\boldsymbol{\Phi} = -m_A \boldsymbol{\gamma} + (m_A + \rho|\Omega_S|)\ddot{\mathbf{U}}_F$. The confinement ratio B_S is finally obtained from the equation $B_S = ((m_a + \rho|\Omega_S|)/(m_a + \rho(|\Omega_S| + |\Omega_T|)))$. For the geometry under concern here, calculation leads to $B_S = 0.7752$.

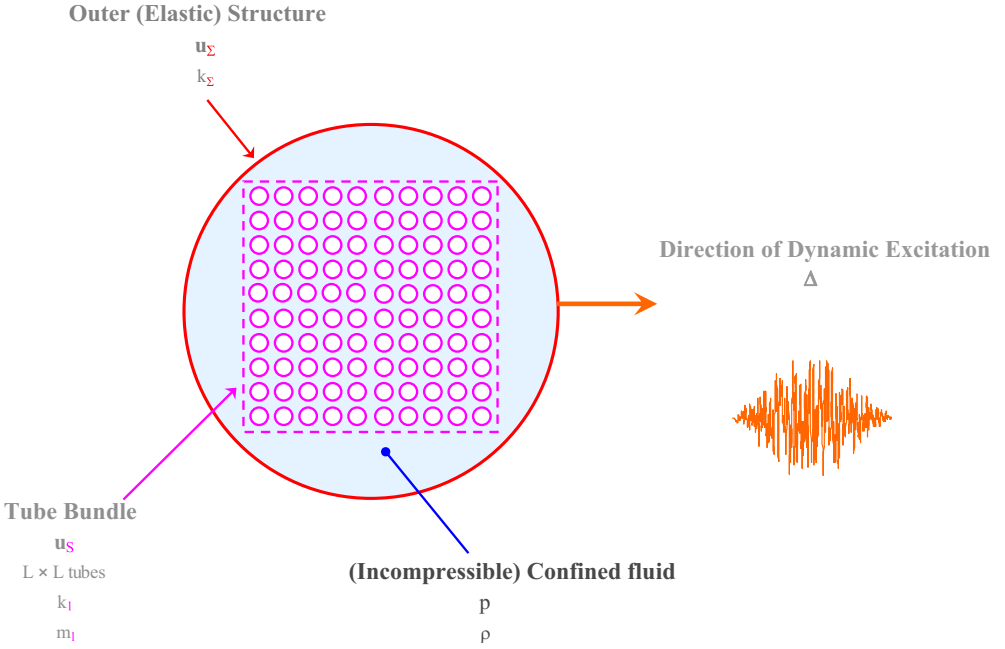

Fig. 5. 10×10 tube bundle system embedded within a circular elastic structure.

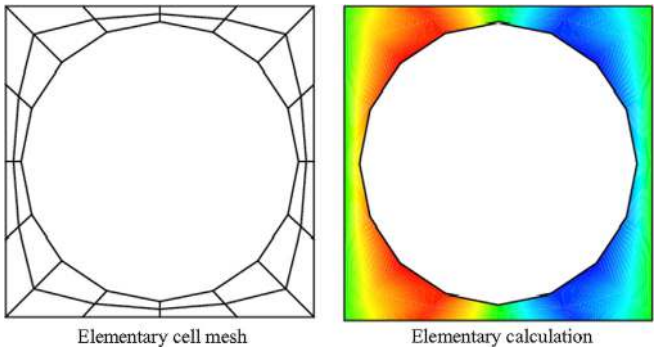

Fig. 6. Elementary cell mesh and elementary pressure field calculation.

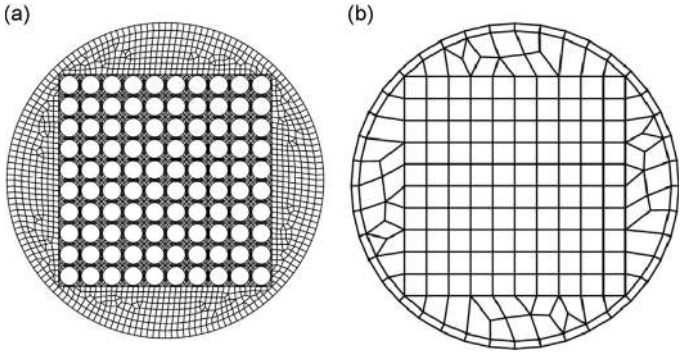

Fig. 7. Finite element mesh of the 10×10 tube bundle: (a) coupled method and (b) homogenisation method.

Table 1
Comparison of coupled and homogenised methods in terms of computation cost.

	Coupled	Homogenised
Computation time [s]	2150	295
Number of nodes	6700	660
Problem size [non-dimensional]	21,000	3500

3.2. Upper and lower bound of tubes/fluid eigenfrequencies

Calculations of eigenmodes and eigenfrequencies together with the effective mass of the tube bundle are performed with the "classical method" – i.e. based on the finite element discretisation of the structure, tubes and fluid "classical" equations – and with the "homogenised method"; Fig. 7 highlights the differences between the two methods in terms of finite element mesh of the coupled system: using the homogenised method obviously reduces the size of the problem (see also Table 1).

As stated above, eigenfrequencies of the tubes system in vacuum have the same value for all modes. When coupled with the fluid, inertial effects arise and are characterised as follows. Motion of the tubes induces fluid flow, the latter gaining kinetic energy which depends on the tubes motion pattern.

- Fluid kinetic energy, hence inertial effect, is maximum when no global flux is observed between two adjacent cells, i.e. when the confinement of the tube in the cell is maximum (in this case, $\ddot{\mathbf{U}}_F = \mathbf{0}$). Using Eq. (2), the force on the tube is calculated as $\mathbf{\Phi} = -m_a \ddot{\mathbf{u}}_S$, which yields a lower bound for the frequencies of the tubes with fluid $f_{min} = f_o/\sqrt{1+(m/m_a)} < f_o$,
- Fluid kinetic energy, hence inertial effect, is minimum when the fluid and the tubes move in the same direction, i.e. when the tubes offer no resistance to the fluid flow (in this case, $\nabla p = 0$). Using Eq. (5), the force on the tube is calculated as $\mathbf{\Phi} = -m_a^* \ddot{\mathbf{u}}_S$, which yields an upper bound for the frequencies of the tubes with fluid $f_{max} = f_o/\sqrt{1+(m/m_a^*)} < f_o$.

The eigenfrequencies of the tubes and fluid system are therefore found to lie within the frequency range $[f_{min}, f_{max}]$. Calculations performed both with "classical" and "homogenised" methods are compared in Fig. 8 in terms of cumulated effective mass and number of modes versus the reduced eigenfrequencies ($\beta = f/f_o$) of the tube bundle. Both methods yield

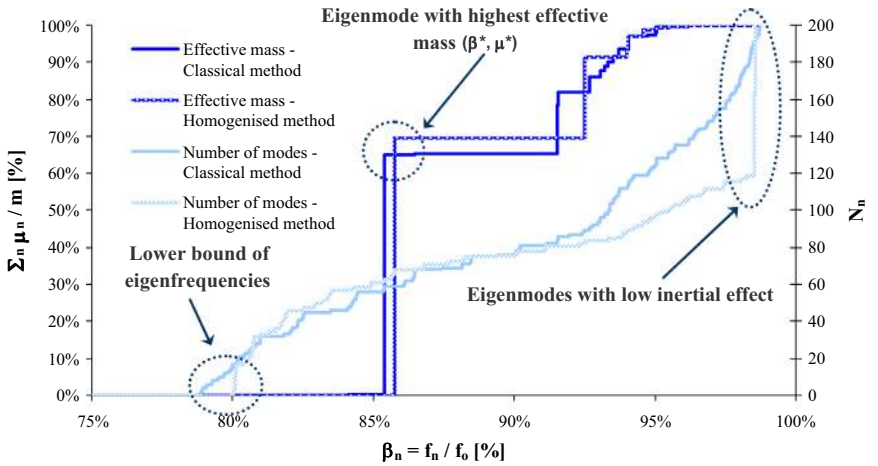

Fig. 8. Comparison of the "classical" and "homogenised" methods: effective masses and number of modes.

Table 2
Comparison of coupled and homogenised methods in terms of calculation of the frequency range of the spectrum for the elementary tube bundle.

Frequency ratio	Coupled	Homogenised
$\beta_{\min}$ [%]	79.28	80.28
$\beta_{\max}$ [%]	98.75	98.50

a lower and a upper bound of the eigenfrequencies, with some discrepancies (see Table 2), which can be accounted for as follows.

In the low frequency range, an added mass is evaluated with the "classical" and "homogenised" representations: denoted $m_a^{Classical}$ and $m_a^{Homogenised}$, they differ from the theoretical value m_a. Assuming that there is no interaction between tubes of adjacent cell, and considering the case of a maximum confinement for the tube in the cell:

- the "classical" representation corresponds to an elementary calculation with boundary conditions $\partial p/\partial n = 0$ on $\Gamma_{F\pi}$ and Γ_{Fo}, which is equivalent to having $\ddot{\mathbf{U}}_F = \mathbf{0}$ (no global flux) and $\ddot{\mathbf{u}}_F \equiv \mathbf{0}$ (no local flow) at the cell outer boundary,
- the "homogenised" representation corresponds to an elementary calculation with boundary conditions $\partial p/\partial n = 0$ on $\Gamma_{F\pi}$ and $p = 0$ on Γ_{Fo}, which is equivalent to considering $\ddot{\mathbf{U}}_F = \mathbf{0}$ (no global flux) but not $\ddot{\mathbf{u}}_F \equiv \mathbf{0}$ (some fluid can flow from one cell to another) at the cell outer boundary.

Confinement being higher with the "classical" representation, it follows that $m_a^{Classical} > m_a^{Homogenised}$; hence, $\beta_{min}^{Classical} < \beta_{min}^{Homogenised}$, as observed in Table 2.

In the same manner, the "classical" and "homogenised" representations yield an added mass in the high frequency range which differs from the theoretical value m_a^*. They are denoted as $m_a^{*Classical}$ and $m_a^{*Homogenised}$, with $m_a^{*Classical} < m_a^{*Homogenised}$; hence, $\beta_{\max}^{\text{Classical}} > \beta_{\max}^{\text{Homogenised}}$, as observed in Table 2.

Fig. 9 gives a representation of the coupled eigenmode with the highest effective mass, obtained through calculation with the "classical" method on one hand and the "homogenised" method on the other. Agreement between the two approaches is remarkable both qualitatively (mode shape) and quantitatively (frequency, effective mass).

3.3. Accuracy of the method for low inertial effects

For the mode depicted in Fig. 9, the inertial effect is high and the small scale variations of the displacement/pressure fields are low, so that the physics is in accordance with underlying assumptions of the homogenisation. Although no discrepancies are noticeable for other modes with high inertial effects, some differences arise for modes with low inertial effects. The homogenisation approach fails to accurately calculate the eigenfrequencies for such modes since all computed modes have an identical eigenfrequency.

This shortcoming of the method is of no importance when linear dynamic analysis of the system subjected to seismic loading is concerned. Indeed the modes of concern have low effective mass and their contribution to the global behaviour of the system can be neglected.

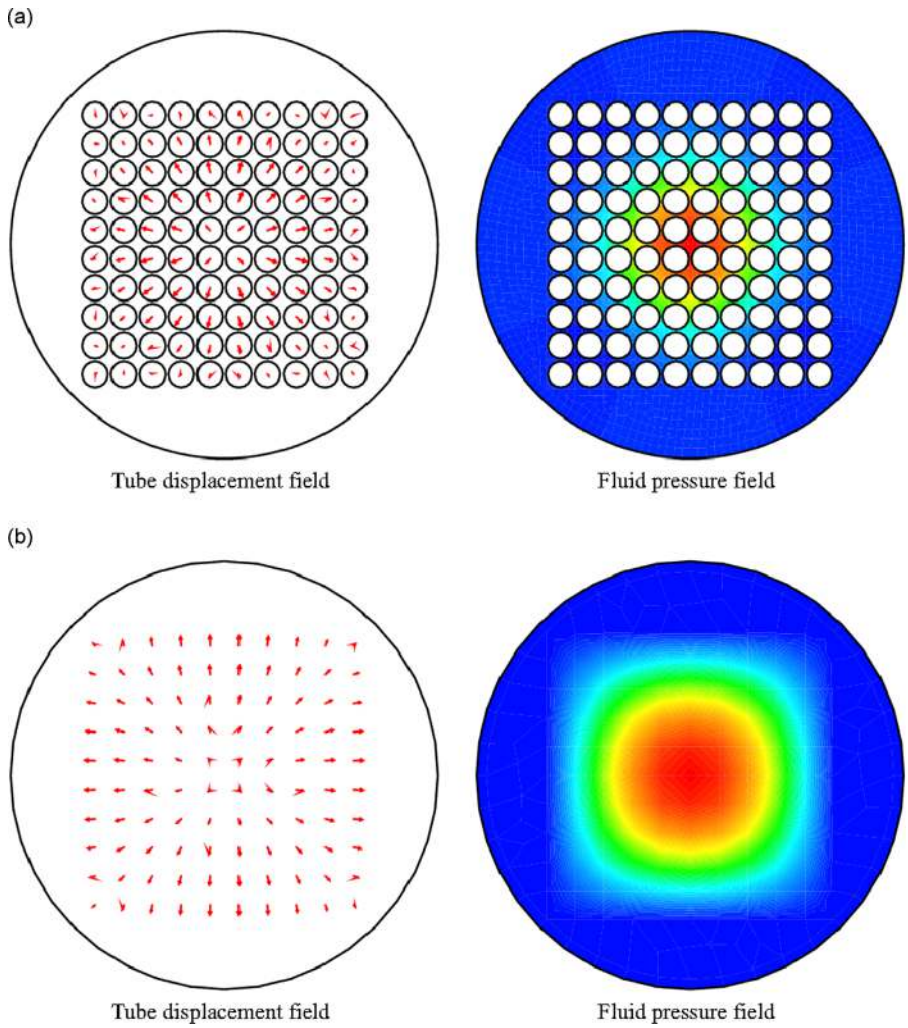

Fig. 9. Comparison of "classical" and "homogenised" methods: eigenmodes with highest effective mass (β is the ratio of the mode frequency to the frequency of a single tube in vaccum, μ is the ratio of the mode effective mass to the total mass of the system – i.e. structure, fluid and tubes mass): (a) "classical" method – $\beta = 80.41\%$ (frequency), $\mu = 34.3\%$ (effective mass) and (b) "homogenised" method – $\beta = 80.3\%$ (frequency), $\mu = 31.7\%$ (effective mass).

It is however no longer the case when non-linear effects (such as impacts between tubes) are taken into account in the analysis: enhancement of the homogenised representation is therefore needed to handle such situations.

4. Modelling of interaction between tubes

4.1. 1-D interaction model

As highlighted in the introduction, one underlying hypothesis of the proposed homogenisation approach is that "interactions between neighbouring tubes are not taken into account". This assumption implies that the fluid kinetic energy generated by the local motion of adjacent tubes is rendered in Eqs. (6) and (7).

Eigenmodes with low inertial effects are characterised by interactions between neighbouring tubes, and the homogenisation method fails to adequately describe FSI for such modes. Assembling the dynamic equations of the homogenised system accounts for interaction between cells, but under the assumption of a repetitive pattern from one cell to another. This holds when acceleration of the tubes does not vary significantly from one cell to another. As emphasized in Fig. 8 and as illustrated in Fig. 9, this way of modelling tube interactions holds only for "global modes" of the tubes system. Higher order modes involve local motion which gives rise to different relative tube displacements from one cell to the other. The kinetic energy which is generated by such interactions is not accounted for.

In order to highlight the consequence of this assumption, let us first consider a row of square tubes in square confinement. The problem is limited to 1D, for the sake of clarity (see Fig. 10). All tubes have identical mass and stiffness properties m and k; the natural frequency of each tube is f_o.

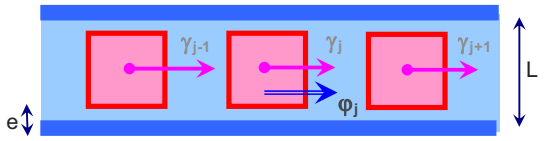

Fig. 10. 1D square tube array in square confinement.

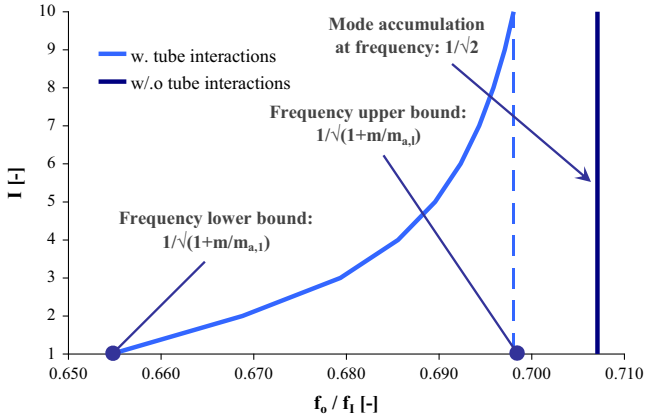

Fig. 11. Evidencing the mode accumulation for the 1D square tube array.

To begin with, the interaction between tubes is not accounted for. According to Cheval (2001), an analytical calculation of the force acting on tube i is possible. It is found to be $\varphi_i = -(\rho L^3/e)\gamma_i$, where γ_i is the tube acceleration; hence, all tubes have an identical added mass $m_a = \rho L^3/e$.

When the interaction between tubes is taken into account, following once again Cheval (2001), the fluid force on tube i is calculated as

$$\varphi_i = -\frac{\rho L^3}{e}\gamma_i + \frac{\rho L^3}{12e}(\gamma_{i-1} - 2\gamma_i + \gamma_{i+1}) \tag{10}$$

Let us now consider a vibration mode of a set of $I+1$ tubes, such that $\gamma_i = \cos(i\pi/I)$ for all $i \in [0, I]$; the force on tube i is readily

$\varphi_i = -(\rho L^3/e)\cos(i\pi/I) + (\rho L^3/12e)(\cos((i-1)\pi/I) - 2\cos(i\pi/I) + \cos((i+1)\pi/I))$ which is also $\varphi_i = -(\rho L^3/e)\cos(i\pi/I)(1+\sin^2(\pi/2I)/3)$, so that the added mass on any tube is $m_a^I = (\rho L^3/e)(1+\sin^2(\pi/2I)/3)$.

- For $I = 1$, the tubes vibrate according to an "out-of-phase" motion: the elementary pattern in the mode shape is $-1, +1$. The inertial effects are maximised. The corresponding added mass is $m_a^1 = 4\rho L^3/3e$; hence the lower bound of the coupled eigenfrequencies is evaluated as $f_{min} = f_o/\sqrt{1+(m/m_a^1)}$.
- For $I = 2$, the tubes vibrate according to a periodic shape $-1, 0, +1, 0$ and the added mass is $m_a^2 = 7\rho L^3/6e$. For $I = 3$, the tubes vibrate according to a periodic shape $-1, -1/2, 1/2, 1, 1/2, -1/2$, and the added mass is $m_a^2 = 13\rho L^3/12e$.
- For $I \to \infty$, the tubes vibrate according to an "in-phase" motion, the inertial effects are minimised and the added mass is $m_a^\infty = \rho L^3/e$, which corresponds to the case where no interaction occurs between tubes. This gives the upper bound of the coupled eigenfrequencies: $f_{max} = f_o/\sqrt{1+(m/m_a^\infty)}$.

Considering a system of I identical tubes and discarding the tubes interaction give I modes with the same eigenfrequency $f = f_o/\sqrt{1+(m/m_a)}$; therefore an "accumulation" of modes is observed; modelling the tubes interaction yields I modes with frequencies $f \in [f_o/\sqrt{1+(m/m_a^1)}, f_o/\sqrt{1+(m/m_a^I)}]$ as presented in Fig. 11 for I=10 tubes (for the sake of convenience, it is assumed that $m = m_a = 1$).

In the 2-D case for a circular tube in square confinement, an accumulation is also observed for low inertial effect eigenmodes at the same frequency, as highlighted in Fig. 8, while the high inertial effect eigenmodes are correctly accounted for. Thus it is expected that taking tubes interaction into account will improve the representation of the "accumulated modes".

4.2. 2-D interaction model

The case of a circular tube in a square confinement is considered here, although the same approach could be employed for other situations.

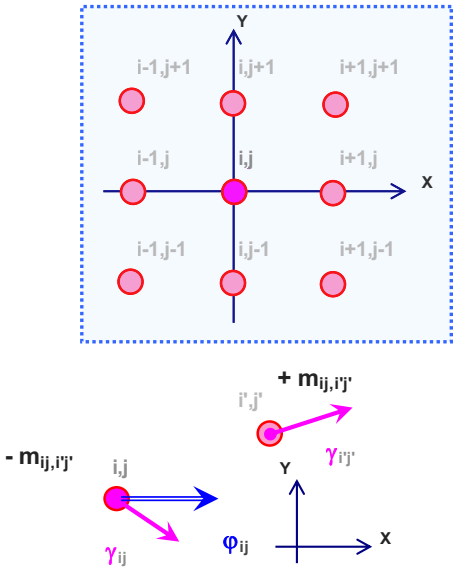

Fig. 12. 2D tube array: one tube/eight neighbouring tubes and interactions between two tubes.

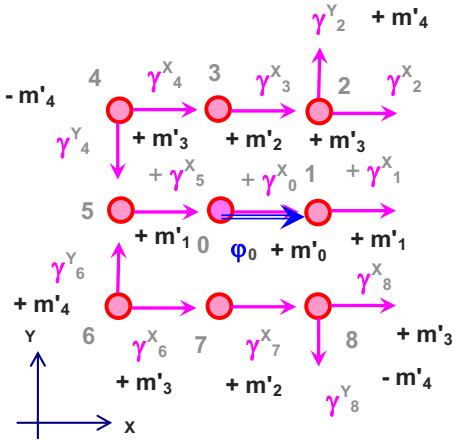

Fig. 13. Interactions between tubes: definition of corrective terms.

Eq. (10) takes into account the interaction of tube i with tubes $i-1$ and $i+1$ through a corrective term which can be calculated as $-(\rho L^3/12e)(\gamma_i-\gamma_{i-1})-(\rho L^3/12e)(\gamma_i-\gamma_{i+1})$, so that the interaction between tube i and $i+1$ is described through a fluid force $\varphi_{i+1\to i}=-m_c(\ddot{u}_i-\ddot{u}_{i+1})$, with $m_c=\rho L^3/12e$; hence, the kinetic energy generated in the fluid by the interaction between tube i and $i+1$ is $(1/2)\ddot{\mathbf{U}}^T\mathbf{M}_C^{i,i+1}\ddot{\mathbf{U}}$, with $\mathbf{M}_C^{i,i+1}=-\begin{bmatrix}+m_c & -m_c\\ -m_c & +m_c\end{bmatrix}\begin{matrix}i\\ i+1\end{matrix}$.
$\qquad\qquad\quad i \quad i+1$

In the 2-D case for a tube in a square confinement, let us consider the interaction of a tube with its eight neighbours, see Fig. 12. Interactions of the central tube with the others are described with fluid force $\varphi_{ij}=\sum_{\substack{i'=i-1,i(j'\neq j),i+1\\ j'=j-1,j,j+1}} -m_{ij,i'j'}^{XY}(\gamma_{ij}^{XY}-\gamma_{i'j'}^{XY})$ in the directions X and Y, which can be seen as a corrective force to account for tube interactions.

The interaction matrix $[m_{ij,i'j'}^{X,Y}]$ is composed of 16 terms (interaction of each tube with eight other tubes in two directions). However, because of symmetries within the nine tubes system, only five terms have to be calculated. According to notations of Fig. 13, fluid force on the central tube is given by

$$\varphi_0=+m'_0\gamma_0^X+m'_1(\gamma_1^X+\gamma_5^X)+m'_2(\gamma_3^X+\gamma_7^X)+m'_3(\gamma_2^X+\gamma_4^X+\gamma_6^X+\gamma_8^X)+m'_4(\gamma_2^Y-\gamma_4^Y+\gamma_6^Y-\gamma_8^Y).$$

m'_0, m'_1, m'_2, m'_3 and m'_4 are calculated with five elementary calculations, through the analysis of simple vibration modes for the bundle. The analysis of each mode is reduced to only one cell with one tube. The fluid flow and the forces applied to

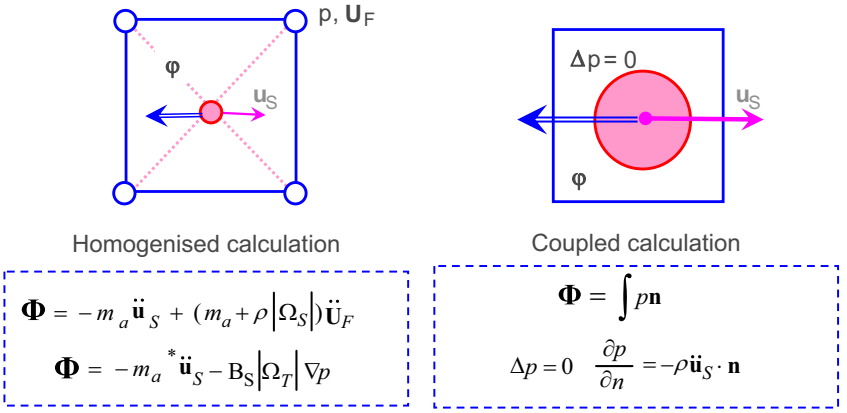

Fig. 14. Homogenised and classical calculation on elementary cell.

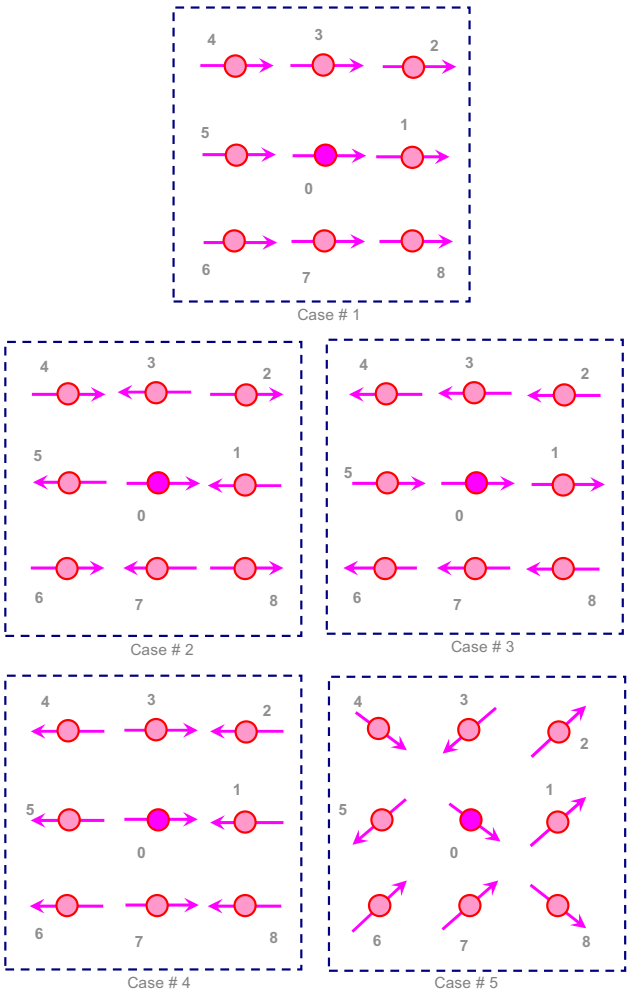

Fig. 15. Definition of five elementary cases for determining the m' coefficients.

the tube is calculated by the difference between a "classical" and "homogenised" calculation (see Fig. 14): the corrective force is obtained from the difference between the results obtained with the two methods. A linear equation in terms of m'_0, m'_1, m'_2, m'_3 and m'_4 is derived from the correction. These coefficients depend on the geometry under concern: for a tube in square confinement, they are obtained from the study of five different vibration cases (see Fig. 15), as detailed below.

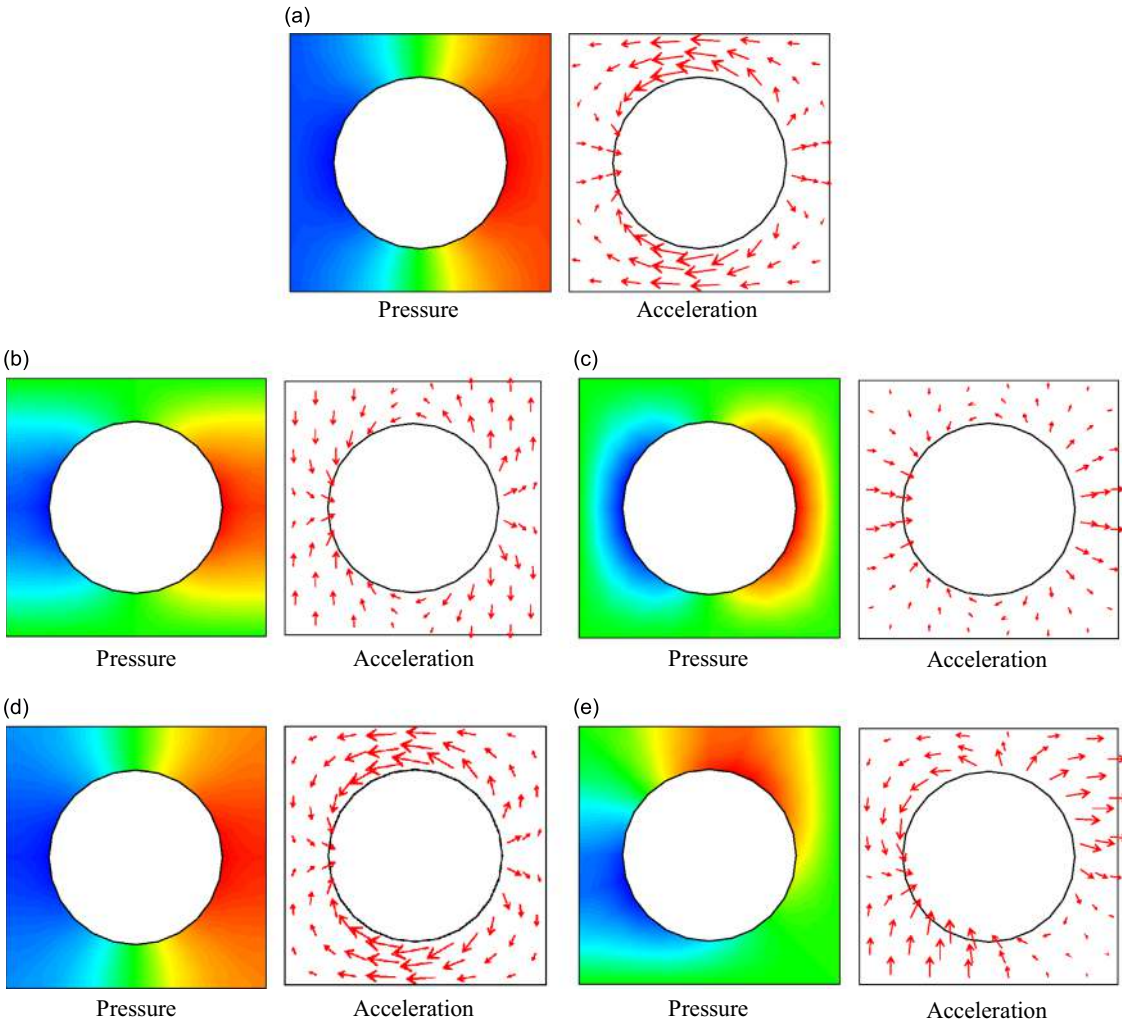

Fig. 16. Pressure and acceleration field in the fluid-tube cell for the five elementary cases: (a) 1, (b) 2, (c) 3, (d) 4, and (e) 5.

Case #1 corresponds to the situation where all the tubes of the bundle have the same acceleration γ, with a global fluid flow equal to zero. The pressure and acceleration fields in the elementary cell are depicted in Fig. 16(a). In this case the homogenisation method gives exact forces applied to each tube, $-m_a\gamma$. The corrective force, given by $m'_0+2m'_1+2m'_2+4m'_3$, is therefore null. The tube interaction forces deal with local effects and do not influence the global fluid flow in the bundle. This yields the first linear relations for the m' coefficients: $m'_0+2m'_1+2m'_2+4m'_3=0$.

Cases #2–4 correspond to vibration modes with various symmetry/anti-symmetry conditions, as detailed in Table 3. The pressure and acceleration fields in the elementary cell are depicted in Fig. 16(b)–(d). Detailed calculation of the corrective forces is as follows.

- For case #2, the force applied to the tube evaluated with the coupled calculation is -778.85γ, while the force applied to the tube with the homogenisation method is -373.32γ. The corrective force is $+405.53\gamma$ and the second linear relation is $-m'_0+2m'_1+2m'_2-4m'_3=-405.53$.
- For case #3, the coupled calculation gives the force -344.92γ, while homogenised method yields -373.32γ. The corrective force is -28.40γ; hence $-m'_0-2m'_1+2m'_2+4m'_3=-28.40$.
- For case #4, the fluid forces are -1667.70γ (coupled calculation) and -1574.90γ (homogenised calculation); the fourth linear relation is then $-m'_0+2m'_1-2m'_2+4m'_3=-102.80$.

Finally, case #5 yields the last relation as $-m'_0-4m'_3=-175.82$, which corresponds to the vibration mode depicted in Fig. 16(e), with calculation of the fluid force as -549.14γ and -373.32γ, respectively, with the coupled and homogenised methods.

Table 3
Symmetry conditions an boundary conditions for elementary cases #2–4.

Case	*X* direction	*Y* direction	Lower/upper boundaries	Lateral boundaries
♯2	Anti-symmetry	Anti-symmetry	$p=0$	$p=0$
♯3	Symmetry	Anti-symmetry	$\frac{\partial p}{\partial n}=0$	$p=0$
♯4	Symmetry	Symmetry	$\frac{\partial p}{\partial n}=0$	$\frac{\partial p}{\partial n}=0$

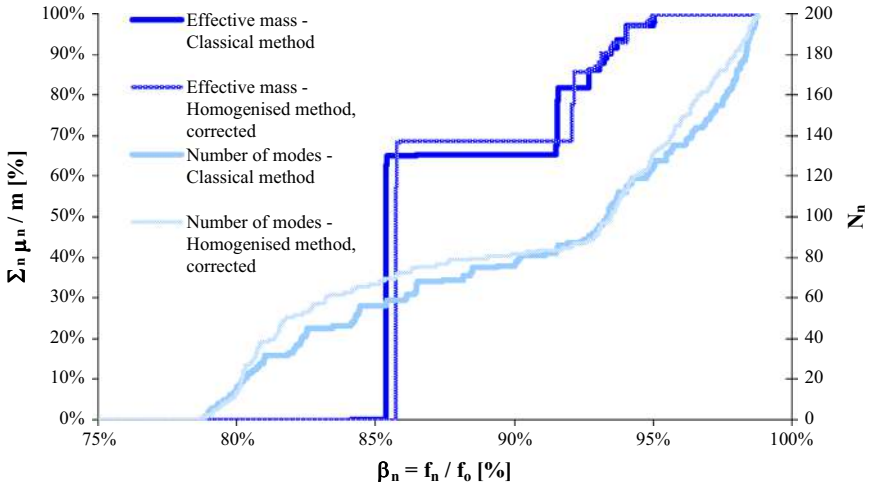

Fig. 17. Comparison of the "classical" and "corrected homogenised" methods: effective masses and number of modes.

Once calculated, the five coefficients define an elementary "corrected added mass" matrix for each tube. Assembling these elementary matrices yields a global "corrected added mass" matrix $\mathbf{M}_C$ which is introduced in the general formulation of the coupled problem; Eq. (9) is thereby modified as

$$\begin{bmatrix} \mathbf{M}_S+\mathbf{M}_S^*+\mathbf{M}_C & \mathbf{0} & \mathbf{0} & -\rho B_S\mathbf{C} \\ \mathbf{0} & \mathbf{M}_\Sigma & \mathbf{0} & \rho\mathbf{R} \\ \mathbf{0} & \mathbf{0} & \mathbf{0} & \overline{\mathbf{M}}_F \\ -\rho B_S\mathbf{C}^{\mathrm{T}} & \rho\mathbf{R}^{\mathrm{T}} & \overline{\mathbf{M}}_F & -\rho(1-B_S)\mathbf{K}_F \end{bmatrix} \begin{Bmatrix} \ddot{\mathbf{U}}_S(t) \\ \ddot{\mathbf{U}}_\Sigma(t) \\ \ddot{\mathbf{P}}(t) \\ \ddot{\mathbf{\Phi}}(t) \end{Bmatrix} + \begin{bmatrix} \mathbf{K}_S & \mathbf{0} & \mathbf{0} & \mathbf{0} \\ \mathbf{0} & \mathbf{K}_\Sigma & \mathbf{0} & \mathbf{0} \\ \mathbf{0} & \mathbf{0} & 1/\rho\overline{\mathbf{M}}_F & \mathbf{0} \\ \mathbf{0} & \mathbf{0} & \mathbf{0} & \mathbf{0} \end{bmatrix} \begin{Bmatrix} \mathbf{U}_S(t) \\ \mathbf{U}_\Sigma(t) \\ \mathbf{P}(t) \\ \mathbf{\Phi}(t) \end{Bmatrix} = \begin{Bmatrix} \mathbf{0} \\ \mathbf{0} \\ \mathbf{0} \\ \mathbf{0} \end{Bmatrix}. \tag{11}$$

4.3. Application for the 10 × 10 2-D tube bundle

Using a corrective matrix which accounts for the interaction of adjacent tubes is expected to improve the ability of the homogenisation method to describe the dynamic behaviour of a tube bundle. Application of the "corrected homogenised" method is carried out on the 10×10 tube bundle as depicted in Fig. 5. A modal analysis is performed with the "homogenised" and "corrected homogenised" methods. Comparison of the homogenised methods and the coupled method is shown through the calculation of the effective mass, which characterises the seismic behaviour of the system, and its eigenfrequencies.

Fig. 17 compares the numerical results with those given by a modal analysis using the "classical" method. As far as the effective mass is concerned, the agreement between both approaches is fairly good. The correction introduced in the "homogenised" technique improves the precision of the modal effective masses but differences between the "uncorrected" and "corrected" homogenisation approaches, when compared to the "classical" approach, are not obvious. Improvements are more significant when it comes to predicting the repartition of eigenmodes throughout the spectrum of the tube bundle. As presented in Fig. 18, the number of modes versus frequency curve obtained with the "corrected homogenised method" is in good qualitative agreement with the one obtained with the "classical" method, especially as far as coupled modes with low inertial effects are concerned. Comparison of the number of modes calculated over the $[f_{min},f_{max}]$ frequency range with the "classical" and the "homogenised" methods (with and without corrective terms) is proposed in Fig. 14. It clearly emphasises the influence of tube interactions for modes close to f_{max}.

A more quantitative comparison is obtained by calculating the "correlation matrix" of modal bases $\mathbf{\Phi}_c$ ("classical" method) and $\mathbf{\Phi}_h$ ("homogenised" method). By definition, it is calculated according to $\mathbf{\Phi}_c^T\mathbf{\Phi}_h/\sqrt{\mathbf{\Phi}_c^T\mathbf{\Phi}_c}\sqrt{\mathbf{\Phi}_h^T\mathbf{\Phi}_h}$: the closer to

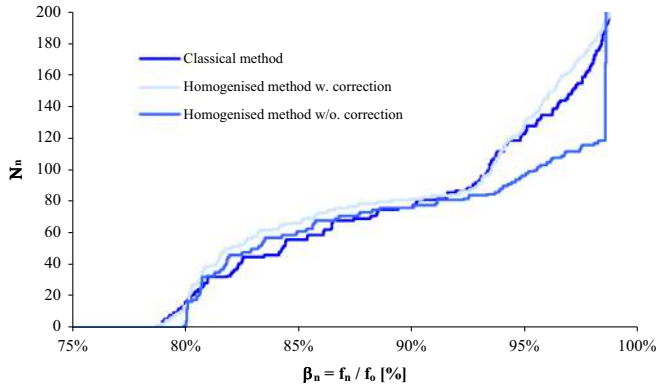

Fig. 18. Comparison of the "classical" method and "homogenised" method with and without correction: number of modes.

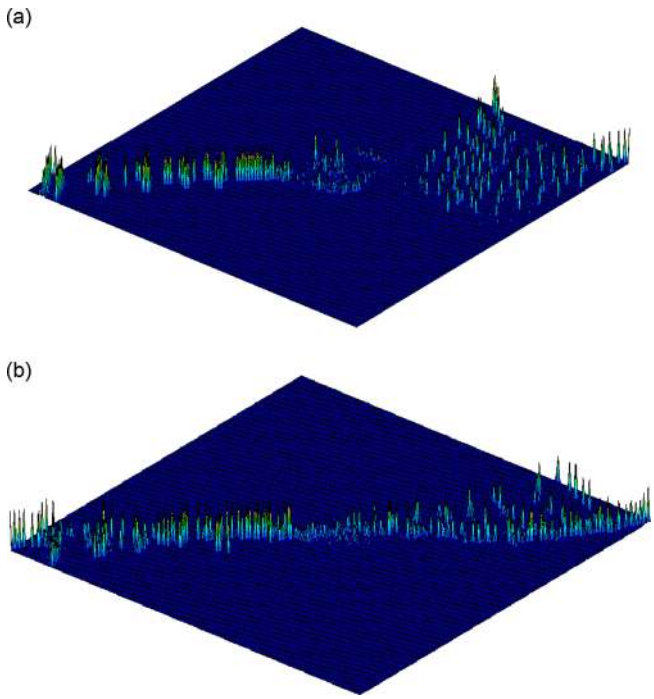

Fig. 19. Correlation matrices: "classical" modes versus "homogenised" modes: (a) correlation of "classical" and "homogenised" modes – without correction and (b) correlation of "classical" and "homogenised" modes – with correction.

the unity diagonal, the better the correlation of modal bases (Allemang, 2003). Fig. 19 gives the correlation matrices of "classical" and "homogenised" methods with and without correction and illustrates the improvement trends observed in Fig. 18.

5. Conclusion

A homogenisation method has been developed in order to perform the dynamic analysis of a tube bundle with fluid–structure interaction modelling using modal methods. It is concerned with the description of inertial effects which predominate in the low frequency range, for small displacement of the tubes when immersed in a fluid, supposed non-viscous and incompressible. It is based on the description of the tubes–fluid system through an equivalent continuous medium, characterised by a set of dynamic equations which describe the behaviour of the tubes and the fluid from a global point of view. Based on physical consideration, the interaction between fluid and tubes is accounted for at the local scale using a two degrees of freedom system.

Mathematical formulation of the proposed method has been shown and discussed from the physical point of view. From the numerical perspective, the discretisation of the coupled equation can be performed with a finite element technique, which enables possible industrial applications. The ability of the method to accurately account for inertial effects has been discussed on a simple 2D test-case, namely a 10×10 tube array immersed in a fluid. The limits of the homogenised model have been identified and discussed using physical considerations.

The underlying hypothesis of the method has also been clarified: taking into account the interactions between the tubes allows for a more accurate description of inertial effects for particular modes of the tubes and fluid system. Accordingly, a correction of the homogenisation method has been proposed by introducing some inertial terms in the model. This correction improves the representation of "low inertial effects" eigenmodes, without burdening the overall modelling procedure. This approach opens a path for applications of the method to a wider range of problems encountered in the nuclear industry.

Description of inertial effects in a tube bundle still remains as an open problem to some extent. Future work will focus on some physical as well as mathematical aspects of the method. Additional FSI effects are also of importance when modelling the behaviour of periodic fluid–structure systems. For instance, taking into account viscous effects for the fluid and/or large displacement of the tube might be of interest. To that end, an extension of the present methodology to the homogenisation approach on the Navier–Stokes equations should be proven worthy. A first contribution is proposed in Desbonnets and Broc (2012) and offers some perspectives to extend the present homogenisation model in tube bundles.

Acknowledgement

The authors gratefully acknowledge MM. Belmere and Lopez at CEA for their continuous support to the scientific collaboration between DCNS Research and CEA Saclay in fluid–structure interaction modelling applied to nuclear propulsion systems.

References

Allemang, R.J., 2003. The modal assurance criterion. Twenty years of use and abuse. Sound and Vibration Magazine, 14–20.
Axisa, F., Antunes, J., 2006. Modelling of Mechanical Systems. Fluid–Structure Interaction, vol. 3. Elsevier, Oxford.
Bensoussan, A., Lions, J.L., Papanicolaou, G., 1978. Asymptotic Analysis for Periodic Structures. North-Holland, Amsterdam.
Broc, D., Queval, J.C., Viallet, E., 2003. Seismic behaviour of PWR reactor cores: fluid–structure effects. In: Proceedings of the 17th Conference on Structural Mechanics in Reactor Technology, Prague.
Brochard, D., Gantenbein, F., Gibert, R.J., 1987a. Homogenisation of tube bundle. Application to LMFBR core analysis. In: Proceedings of the 9th Conference on Structural Mechanic in Reactor Technology, Lausanne.
Brochard, D., Gantenbein, F., Gibert, R.J., 1987b. Modelling of the dynamic behaviour of LWR internals. In: Proceedings of the 9th Conference on Structural Mechanics in Reactor Technology, Lausanne.
Brochard, D., Jedrzajewski, F., Gibert, R.J., Le Moal, D., 1996. 3D Analysis of the Fluid Structure Interaction in Tube Bundle Using Homogenisation Methods, vol. 337. American Society of Mechanical Engineers, Pressure Vessel and Piping Division (Publication)167–171.
Cheval, K., 2001. Modélisation du comportement sismique de structures multitubulaires baignées par un fluide dense (Ph.D. thesis). Université Paris VI.
Conca, C., Planchard, J., Vanninathan, M., 1995. Fluids and Periodic Structures. Masson, Paris.
De Ridder, J., Degroote, J., Van Tichelen, K., Schuurmans, P., Vierendeels, J., 2013. Modal characteristics of flexible cylinder in turbulent axial flow from numerical simulations. Journal of Fluids and Structures 43, 110–123.
Desbonnets, Q., Broc, D., 2012. Homogenisation method for the vibration of tube bundle in a fluid. In: Proceedings of the 10th Flow-Induced Vibration Conference, Dublin.
Gallardo, D., Bevilacqua, R., Sahni, O., 2014. Data-based hybrid reduced order modeling for vortex-induced non-linear fluid structure interaction at low Reynolds numbers. Journal of Fluids and Structures 44, 115–128.
Hammami, L., 1991. Etude de l'interaction fluide/structure dans les faisceaux de tubes par une méthode d'homogénéisation. Application à l'analyse sismique des cœurs RNR (Ph.D. thesis). Université Paris VI.
Jacquelin, E., Brochard, D., Trollat, C., Jézéquel, L., 1996. Homogenisation of non-linear array of confined beams. Nuclear Engineering and Design 165, 213–223.
Morand, H.-J.P., Ohayon, R., 1995. Fluid–Structure Interaction. Wiley & Sons, Chichester.
Planchard, J., 1985a. Vibration of nuclear fuel assemblies: a simplified model. Nuclear Engineering and Design 86, 383–391.
Planchard, J., 1985b. Modelling the dynamic behaviour of nuclear reactor fuel assemblies. Nuclear Engineering and Design 90, 331–339.
Planchard, J., 1987. Global behaviour of large elastic tube bundle immersed in a fluid. Computational Mechanics 2, 105–118.
Sanchez-Palencia, E., 1980. Non Homogenous Media and Vibration Theory. Springer-Verlag, Berlin.
Schumann, U., 1981. Homogenised equations of motion for rod bundle in the fluid with periodic structure. Ingenieur-Archiv 50, 203–216.
Shinohara, Y., Shimogo, T., 1981. Vibrations of square and hexagonal cylinders in a liquid. Journal of Pressure Vessel Technology 103, 233–239.
Sigrist, J.F., Garreau, S., 2007. Dynamic analysis of fluid–structure interaction problems with spectral method using pressure-based finite elements. Finite Element Analysis in Design 43, 287–300.
Sigrist, J.F., Broc, D., 2007a. Investigation of numerical methods for modal analysis of tube bundle with fluid–structure interaction. In: Proceedings of the Pressure Vessel and Piping Conference, San Antonio, 22–26 July 2007.
Sigrist, J.F., Broc, D., 2007b. Homogenisation method for the modal analysis of a nuclear reactor with internal structures modelling and fluid–structure interaction coupling. Nuclear Engineering and Design 237, 431–440.
Sigrist, J.F., Broc, D., 2008a. Dynamic analysis of a tube bundle with fluid–structure interaction modelling using a homogenisation method. Computer Methods in Applied Mechanics and Engineering 197, 1080–1099.
Sigrist, J.F., Broc, D., 2008b. Homogenisation method for the modal analysis of tube bundle with fluid–structure interaction modelling. Finite Elements in Analysis and Design 44, 323–333.
Sigrist, J.F., Broc, D., 2009. Fluid–structure interaction modeling for the modal analysis of a steam generator tube bundle. Journal of Pressure Vessel Technology 131. Paper #031302.

Veron, E., Sigrist, J.F., Broc, D., 2014. Implementation of a structural–acoustic homogenised method for the dynamic analysis of a tube bundle with fluid structure interaction modeling within abaqus: formulation and applications. In: Proceedings of the Pressure Vessel and Piping Conference, Anaheim, 20–24 July 2014.
Zhang, R.J., 1998a. Structural homogenised analysis for nuclear reactor core. Nuclear Engineering and Design 183, 151–156.
Zhang, R.J., 1998b. A unified homogenisation mode of beam bundle in fluid. Journal of Pressure Vessel Technology 120, 56–61.
Zhang, R.J., 1999. A beam bundle in a compressible inviscid fluid. Journal of Applied Mechanics 66, 546–548.
Zhang, R.J., Wang, W.Q., Hou, S.H., Chan, C.K., 2001. Seismic analysis of reactor core. Computers & Structures 76, 1395–1404.